

Supporting Information:

A Volume-based Description of Transport in Incompressible Liquid Electrolytes and its Application to Ionic Liquids

Franziska Kilchert,^{†,‡} Martin Lorenz,[¶] Max Schammer,^{†,‡} Pinchas Nürnberg,[¶]
Monika Schönhoff,[¶] Arnulf Latz,^{†,‡,§} and Birger Horstmann^{*,†,‡,§}

[†]*German Aerospace Center, Wilhelm-Runge-Straße 10, 89081 Ulm, Germany*

[‡]*Helmholtz Institute Ulm, Helmholtzstraße 11, 89081 Ulm, Germany*

[¶]*University of Münster, Corrensstraße 28/30, 48149 Münster, Germany*

[§]*Ulm University, Albert-Einstein-Allee 47, 89081 Ulm, Germany*

E-mail: birger.horstmann@dlr.de

Contents

S-1 Theory	S-3
S-1.1 Matrix Form of Onsager Formulation	S-3
S-1.2 Convection Equation	S-3
S-1.3 Reduced Description (Mass-based Frame)	S-4
S-1.4 Derivation of Transformation Rules Between Volume- and Mass-based Reference Frames	S-5
S-1.4.1 Drift Velocities	S-5
S-1.4.2 Species Flux Densities	S-6
S-1.4.3 Electric Current Densities	S-7
S-1.4.4 Transference Numbers	S-7
S-1.5 Derivation of Transformation Rules Between Volume- and Species-based Refer- ence Frames	S-8
S-2 Application to Porous Electrodes	S-9
S-3 Supplementary Data on Application to eNMR Measurements of IL Electrolytes	S-10
S-3.1 Pure Ionic Liquids	S-10
S-3.2 Ionic Liquid + Li-Salt Mixtures	S-12
References	S-15

S-1 Theory

S-1.1 Matrix Form of Onsager Formulation

Equation (S-1) is the matrix formulation of eq. (12) in the mass-based reference frame.

$$\begin{pmatrix} N_2^m \\ \vdots \\ N_N^m \end{pmatrix} = \begin{pmatrix} \mathcal{L}_{22}^m & \cdots & \mathcal{L}_{2N}^m \\ \vdots & \ddots & \vdots \\ \mathcal{L}_{2N}^m & \cdots & \mathcal{L}_{NN}^m \end{pmatrix} \cdot \begin{pmatrix} Fz_2^m \nabla \Phi + \nabla \tilde{\mu}_2^m \\ \vdots \\ Fz_N^m \nabla \Phi + \nabla \tilde{\mu}_N^m \end{pmatrix} \quad (\text{S-1})$$

An equivalent relation can be formulated in the volume-based description for $\mathcal{L}_{\alpha\beta}^v$ by using volume-based species flux densities N_α^v and reduced quantities \tilde{z}_α^v and $\tilde{\mu}_\alpha^v$ (see eq. (21)).

S-1.2 Convection Equation

In Ref. S1, we derived an equation for the drift velocity \mathbf{v}^m . This derivation was based on the fact that the volume is an extensive thermodynamic variable and on the Euler equations for the volume.

Here, we show that our derivation can be applied to different choices for the drift velocity as well. To see this, we consider the variation of the Euler equation for the volume (see eq. (5)), $0 = \sum_{\alpha=1}^N \delta(c_\alpha \nu_\alpha) = \sum_{\alpha=1}^N (\delta c_\alpha \cdot \nu_\alpha + c_\alpha \cdot \delta \nu_\alpha)$. In Ref. S1 we showed that this variation of the Euler equation reduces to concentration variations alone,

$$0 = \sum_{\alpha=1}^N \nu_\alpha \cdot \delta c_\alpha, \quad (\text{S-2})$$

Note that the resulting eq. (S-2) is frame-invariant. However, it can be evaluated with respect to any reference frame via taking the time evolution for the variation $\delta c_\alpha \rightarrow \frac{D^\psi}{dt} c_\alpha = -c_\alpha \nabla \mathbf{v}^\psi - \nabla N_\alpha^\psi$. Here, the frame-dependent derivative operator is defined by $\frac{D^\psi}{dt} = \frac{\partial}{\partial t} + \mathbf{v}^\psi \cdot \nabla$,^{S2} and formalizes the transport equation for the species concentrations. Thus, in the mass description, we find

$$\nabla \mathbf{v}^m = - \sum_{\alpha=1}^N \nu_\alpha \cdot \nabla N_\alpha^m, \quad (\text{S-3})$$

and in the reduced form

$$\nabla \mathbf{v}^m = -\frac{\tilde{\nu}_2^m}{F \tilde{z}_2^m} \nabla J^m - \sum_{\alpha=3}^N \tilde{\nu}_\alpha^m \cdot \nabla N_\alpha^m, \quad (\text{S-4})$$

with

$$\tilde{z}_\alpha^m = z_\alpha - z_1 \cdot M_\alpha / M_1, \quad \tilde{\nu}_\alpha^m = \nu_\alpha - \nu_1 \cdot M_\alpha / M_1, \quad \text{and} \quad \tilde{\tilde{\nu}}_\alpha^m = \tilde{\nu}_\alpha^m - \tilde{\nu}_2^m \cdot \tilde{z}_\alpha^m / \tilde{z}_2^m. \quad (\text{S-5})$$

Whereas in the volume description, we find

$$\nabla \mathbf{v}^v = - \sum_{\alpha=1}^N \nu_\alpha \cdot \nabla N_\alpha^v, \quad (\text{S-6})$$

and in the reduced form

$$\nabla \mathbf{v}^v = -\frac{1}{F} \left(\nu_2 \nabla \frac{J^v}{\tilde{z}_2^v} - \nu_1 \nabla \frac{\nu_2 J^v}{\nu_1 \tilde{z}_2^v} \right) + \sum_{\alpha=3}^N \left(\nu_2 \nabla \frac{\tilde{z}_\alpha^v}{\tilde{z}_2^v} N_\alpha^v - \nu_1 \nabla \frac{\nu_2 \tilde{z}_\alpha^v}{\nu_1 \tilde{z}_2^v} N_\alpha^v - \nu_\alpha \nabla N_\alpha^v + \nu_1 \nabla \frac{\nu_\alpha}{\nu_1} N_\alpha^v \right), \quad (\text{S-7})$$

with

$$\tilde{z}_\alpha^v = z_\alpha - z_1 \cdot \nu_\alpha / \nu_1. \quad (\text{S-8})$$

S-1.3 Reduced Description (Mass-based Frame)

Via mass and charge conservation the number of independent species is reduced by two. From the Euler equation for the volume, eq. (5), follows directly for c_1

$$c_1 = \frac{1}{\nu_1} \left(1 - \nu_2 c_2 - \sum_{\alpha=3}^N \nu_\alpha c_\alpha \right). \quad (\text{S-9})$$

Using this expression together with charge conservation, $q = F \sum_{\alpha=1}^N z_\alpha c_\alpha$, we can determine c_2

$$c_2 = \frac{z_1 - \nu_1 q / F}{\nu_2 z_1 - \nu_1 z_2} + \sum_{\alpha=3}^N c_\alpha \frac{\nu_\alpha z_1 - \nu_1 z_\alpha}{\nu_1 z_2 - \nu_2 z_1}, \quad (\text{S-10})$$

where q is the charge density. Thus, in the electroneutral case ($q = 0$) the charge term vanishes.

S-1.4 Derivation of Transformation Rules Between Volume- and Mass-based Reference Frames

S-1.4.1 Drift Velocities

To obtain the transformation rule for the drift velocities \mathbf{v}^m and \mathbf{v}^v , eq. (27), we start with the basic definitions of the flux densities, eqs. (3) and (6),

$$N_\alpha^m = c_\alpha (\mathbf{v}_\alpha - \mathbf{v}^m) \quad \text{and} \quad N_\alpha^v = c_\alpha (\mathbf{v}_\alpha - \mathbf{v}^v), \quad (\text{S-11})$$

from which we obtain by subtraction

$$N_\alpha^m - N_\alpha^v = c_\alpha (\mathbf{v}^v - \mathbf{v}^m). \quad (\text{S-12})$$

Next, we insert this relation into the flux constraints of the respective reference frames, eqs. (4) and (7), to obtain each side of eq. (27).

$$\sum_{\alpha=1}^N M_\alpha N_\alpha^m = 0 \quad \text{and} \quad \sum_{\alpha=1}^N \nu_\alpha N_\alpha^v = 0 \quad (\text{S-13})$$

$$\sum_{\alpha=1}^N M_\alpha (N_\alpha^v + c_\alpha (\mathbf{v}^v - \mathbf{v}^m)) = 0 \quad \text{and} \quad \sum_{\alpha=1}^N \nu_\alpha (N_\alpha^m + c_\alpha (\mathbf{v}^m - \mathbf{v}^v)) = 0 \quad (\text{S-14})$$

$$\sum_{\alpha=1}^N M_\alpha N_\alpha^v + (\mathbf{v}^v - \mathbf{v}^m) \sum_{\alpha=1}^N M_\alpha c_\alpha = 0 \quad \text{and} \quad \sum_{\alpha=1}^N \nu_\alpha N_\alpha^m + (\mathbf{v}^m - \mathbf{v}^v) \sum_{\alpha=1}^N \nu_\alpha c_\alpha = 0 \quad (\text{S-15})$$

With the relations $\sum_{\alpha=1}^N M_\alpha c_\alpha = \rho$, eq. (2), and $\sum_{\alpha=1}^N \nu_\alpha c_\alpha = 1$, eq. (5), we get

$$\frac{1}{\rho} \sum_{\alpha=1}^N M_\alpha N_\alpha^v = \mathbf{v}^m - \mathbf{v}^v \quad \text{and} \quad \sum_{\alpha=1}^N \nu_\alpha N_\alpha^m = \mathbf{v}^v - \mathbf{v}^m \quad (\text{S-16})$$

Thus,

$$\mathbf{v}^v - \mathbf{v}^m = -\frac{1}{\rho} \sum_{\alpha=1}^N M_\alpha N_\alpha^v = \sum_{\alpha=1}^N \nu_\alpha N_\alpha^m. \quad (\text{S-17})$$

We now reduce the number of flux densities by substituting the first flux density in each case with

$$N_1^v = -\frac{1}{v_1} \sum_{\alpha=2}^N v_\alpha N_\alpha^v \quad \text{and} \quad N_1^m = -\frac{1}{M_1} \sum_{\alpha=2}^N M_\alpha N_\alpha^m, \quad (\text{S-18})$$

respectively. With this, we get

$$\mathbf{v}^v - \mathbf{v}^m = \frac{M_1}{\rho v_1} \sum_{\alpha=2}^N v_\alpha N_\alpha^v - \frac{1}{\rho} \sum_{\alpha=2}^N M_\alpha N_\alpha^v = \sum_{\alpha=2}^N v_\alpha N_\alpha^m - \frac{v_1}{M_1} \sum_{\alpha=2}^N M_\alpha N_\alpha^m, \quad (\text{S-19})$$

$$\mathbf{v}^v - \mathbf{v}^m = \frac{M_1}{\rho v_1} \sum_{\alpha=2}^N \left(v_\alpha - \frac{v_1}{M_1} M_\alpha \right) N_\alpha^v = \sum_{\alpha=2}^N \left(v_\alpha - \frac{v_1}{M_1} M_\alpha \right) N_\alpha^m. \quad (\text{S-20})$$

Finally, we express the term $v_\alpha - \frac{v_1}{M_1} M_\alpha$ as reduced partial molar volumes \tilde{v}_α^m and obtain the transformation rule for the drift velocities as in eq. (27),

$$\mathbf{v}^v - \mathbf{v}^m = \frac{M_1}{\rho v_1} \sum_{\alpha=2}^N \tilde{v}_\alpha^m N_\alpha^v = \sum_{\alpha=2}^N \tilde{v}_\alpha^m N_\alpha^m. \quad (\text{S-21})$$

All following transformation rules can be obtained directly from this equation for the drift velocities.

S-1.4.2 Species Flux Densities

To get the transformation rule for the flux densities as in eq. (29), we make use of the relation between the flux densities and drift velocities, eq. (S-12). Inserting $\mathbf{v}^v - \mathbf{v}^m = \frac{1}{c_\alpha} N_\alpha^m - N_\alpha^v$ for the left side of eq. (S-21) and multiplying with c_α we directly find

$$N_\alpha^m - N_\alpha^v = c_\alpha \frac{M_1}{\rho v_1} \sum_{\beta=2}^N \tilde{v}_\beta^m \cdot N_\beta^v = c_\alpha \sum_{\beta=2}^N \tilde{v}_\beta^m \cdot N_\beta^m. \quad (\text{S-22})$$

S-1.4.3 Electric Current Densities

For the current density transformation rule, eq. (28), we use the relations between the current densities and the drift velocities,

$$J^m = j - q\mathbf{v}^m \quad \text{and} \quad J^v = j - q\mathbf{v}^v, \quad (\text{S-23})$$

where j is the electric current density in the laboratory frame. When solving these relations for \mathbf{v}^m and \mathbf{v}^v , respectively, and inserting them on the left side of eq. (S-21), the laboratory frame current density cancels out. We are left with the transformation rule for the electric current densities

$$J^m - J^v = q \frac{M_1}{\rho v_1} \sum_{\beta=2}^N \tilde{v}_\beta^m \cdot N_\beta^v = q \sum_{\beta=2}^N \tilde{v}_\beta^m \cdot N_\beta^m. \quad (\text{S-24})$$

Here, it becomes obvious that in the electroneutral case where $q = 0$ the electric current densities are invariant under frame transformations and just equal the laboratory frame current density.

S-1.4.4 Transference Numbers

To obtain the transformation rule for the transference numbers, eq. (38), we need the relations between species flux densities and transference numbers,

$$N_\alpha^m = \frac{t_\alpha^m}{Fz_\alpha} J \quad \text{and} \quad N_\alpha^v = \frac{t_\alpha^v}{Fz_\alpha} J. \quad (\text{S-25})$$

Here, we assume electroneutrality ($q = 0$) and J is equal in both relations. Thus, when inserting eq. (S-25) for the flux densities in eq. (S-22) the electric current density and Faraday constant cancel out and we get

$$t_\alpha^m - t_\alpha^v = c_\alpha z_\alpha \frac{M_1}{\rho v_1} \sum_{\beta=2}^N \tilde{v}_\beta^m \frac{t_\beta^v}{z_\beta} = c_\alpha z_\alpha \sum_{\beta=2}^N \tilde{v}_\beta^m \frac{t_\beta^m}{z_\beta}. \quad (\text{S-26})$$

This transformation rule can also be expressed in terms of flux ratios τ_α^m and τ_α^v ,

$$\tau_\alpha^m - \tau_\alpha^v = c_\alpha \frac{M_1}{\rho v_1} \sum_{\beta=2}^N \tilde{v}_\beta^m \tau_\beta^v = c_\alpha \sum_{\beta=2}^N \tilde{v}_\beta^m \tau_\beta^m. \quad (\text{S-27})$$

S-1.5 Derivation of Transformation Rules Between Volume- and Species-based Reference Frames

In the species-based reference frame, one species is designated and in the following this is "species 1". The flux densities N_α^s are, thus, defined relative to that species' drift velocity \mathbf{v}_1 ,

$$N_\alpha^s = c_\alpha (\mathbf{v}_\alpha - \mathbf{v}^s) = c_\alpha (\mathbf{v}_\alpha - \mathbf{v}_1), \quad (\text{S-28})$$

as shown in the main script in eq. (8). Note that in that frame $N_1^s = 0$. Together with the definition for the volume-based flux densities, $N_\alpha^v = c_\alpha (\mathbf{v}_\alpha - \mathbf{v}^v)$ we get

$$\mathbf{v}^v - \mathbf{v}^s = \frac{1}{c_\alpha} (N_\alpha^s - N_\alpha^v) = \mathbf{v}^v - \mathbf{v}_1. \quad (\text{S-29})$$

Multiplying both sides with c_1 yields

$$\frac{c_1}{c_\alpha} (N_\alpha^s - N_\alpha^v) = c_1 (\mathbf{v}^v - \mathbf{v}_1). \quad (\text{S-30})$$

Thus, the N-1 remaining flux densities in the species-based reference frame can be calculated from the volume-based ones via

$$N_\alpha^s = N_\alpha^v - \frac{c_\alpha}{c_1} N_1^v. \quad (\text{S-31})$$

As above, this formulation in terms of flux densities can be readily transformed to transference numbers t_α^s or flux ratios τ_α^s for the electroneutral case via $N_\alpha^s = \frac{\tau_\alpha^s}{F} J = \frac{t_\alpha^s}{F z_\alpha} J$, such that

$$t_\alpha^s = t_\alpha^v - \frac{c_\alpha z_\alpha}{c_1 z_1} t_1^v \quad \text{and} \quad \tau_\alpha^s = \tau_\alpha^v - \frac{c_\alpha}{c_1} \tau_1^v. \quad (\text{S-32})$$

Since the flux density of the designated species N_1^s vanishes by definition, also τ_1^s and t_1^s are zero.

S-2 Application to Porous Electrodes

Many electrochemical applications employ porous electrodes filled with liquid electrolyte. Thus, when applying the theory in volume-averaged physics-based simulations to such electrochemical systems, the set of transport equations must be modified using porous electrode theory^{S3–S6} and species reactions r_α must be taken into account. For this purpose, we assume that the electrolyte is in electroneutral state ($q = 0$) and apply the CM description from Ref. S1 to the volume-based frame,

$$0 = \nabla J_{\text{eff}}^v - F \sum_{\alpha=1}^N z_\alpha r_\alpha, \quad (\text{S-33})$$

$$\partial_t(\epsilon c_\alpha) = -\nabla N_{\text{eff},\alpha}^v - \nabla(\epsilon c_\alpha \mathbf{v}^v) + r_\alpha, \quad \alpha \geq 3, \quad (\text{S-34})$$

$$\partial_t \epsilon = \nabla(\epsilon \mathbf{v}^v) - \sum_{\alpha=1}^N \nu_\alpha r_\alpha. \quad (\text{S-35})$$

Here, the species reactions r_α are incorporated into the transport equations via source terms. The effective species flux densities $N_{\text{eff},\alpha}^v$ and effective current density J_{eff}^v are defined as

$$N_{\text{eff},\alpha}^v = \frac{t_\alpha^{\text{v,red}}}{F \tilde{z}_\alpha^v} J_{\text{eff}}^v - \sum_{\beta=3}^N \epsilon^\beta D_{\alpha\beta}^v \nabla \tilde{\mu}_\beta^v, \quad \alpha \geq 3 \quad (\text{S-36})$$

and

$$J_{\text{eff}}^v = -\epsilon^\beta K^v \nabla \varphi^v - \frac{\epsilon^\beta K^v}{F} \sum_{\beta=3}^N \frac{t_\beta^{\text{v,red}}}{\tilde{z}_\beta^v} \nabla \tilde{\mu}_\beta^v. \quad (\text{S-37})$$

In the above equations, ϵ is the volume fraction of the electrolyte ("porosity"), and β is the Bruggemann coefficient which is related to the tortuosity of the electrode. In the volume-based description, there is no coupling to all species occurring in eq. (S-35). Thus, this description is less numerically challenging compared to the CM-based frame.^{S7}

S-3 Supplementary Data on Application to eNMR Measurements of IL Electrolytes

In table S1 we provide a list with the acronyms of the chemical species used in this work and their full designation.

Table S1: List of chemical acronyms and their full designation.

acronym	full name
BF4	tetrafluoroborate
BMA	butyltrimethylammonium
BMIM	1-butyl-3-methylimidazolium
BmPip	1-butyl-1-methylpiperidinium
EMIM	ethylmethylimidazolium
FSI	bis(fluorosulfonyl)imide
FTFSI	(fluorosulfonyl)(trifluoromethanesulfonyl)imide
PF6	hexafluorophosphate
Pyr12O1	1-methoxyethyl-1-methylpyrrolidinium
Pyr14	1-butyl-1-methylpyrrolidinium
TFSI	bis(trifluoromethylsulfonyl)imide

S-3.1 Pure Ionic Liquids

Table S2 contains the conductivities for all pure ionic liquid (IL) systems measured with impedance spectroscopy as well as the partial molar volumes of each ion calculated from density measurements at 295 K. Conductivities are afflicted with a 10% error and partial molar volumes with 3%. For more details on the experimental specifics we refer to Ref. S8.

Figure S1 shows the mobility ratios against the molar mass ratios according to eq. (49) and complements our argumentation in section 3.3. Apparently, the present ionic liquids (table S2) do not fulfill the mass-based constraint, eq. (49).

Table S2: List of ionic liquids (ILs) with their conductivity and ion partial molar volumes.

IL	conductivity κ S/m	cation partial molar volume v_+ $10^{-6} \text{ m}^3/\text{mol}$	anion partial molar volume v_- $10^{-6} \text{ m}^3/\text{mol}$
EMIM BF4	1.30	110.89	43.70
EMIM TFSI	0.80	107.13	147.26
BMIM TFSI	0.35	145.08	146.25
Pyr14 TFSI	0.23	156.32	145.91
BMA TFSI	0.15	139.71	144.38
BmPip TFSI	0.09	166.46	148.81
BMIM PF6	0.12	144.21	63.10
EMIM FSI	1.52	114.84	87.42
Pyr12O1 FSI	0.63	144.61	91.06

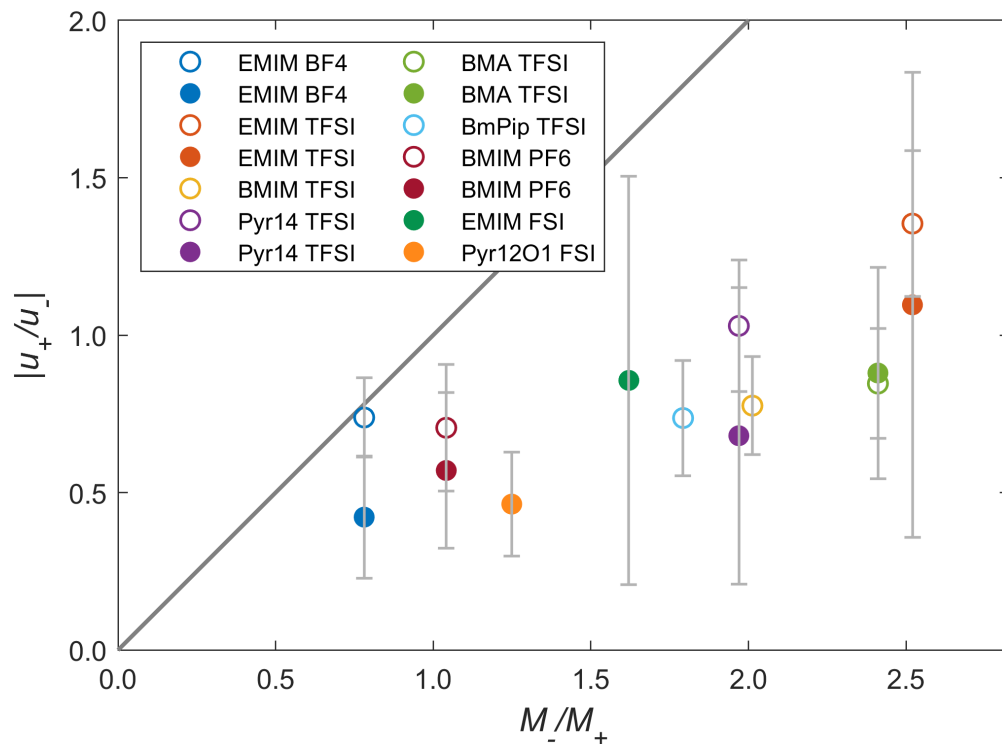


Figure S1: Ratio of mobilities versus ratio of molar masses plotted for various ILs. Open circles: data from Gouverneur et al.;^{S9} Filled circles: data from Lorenz et al.^{S8} Diagonal line: analytical prediction (see eq. (49)).

S-3.2 Ionic Liquid + Li-Salt Mixtures

Table S3 shows a list of the mixtures with three ion constituents and their composition used as database in section 3.4. For the chemical acronyms see table S1.

Table S3: List of mixtures with three ion constituents and their composition.

Sample	Composition	Source
EMIM BF4 1	EMIM BF4 (0.962) Li BF4 (0.038)	Gouverneur 2018 ^{S10}
EMIM BF4 2	EMIM BF4 (0.927) Li BF4 (0.073)	Gouverneur 2018 ^{S10}
EMIM BF4 3	EMIM BF4 (0.86) Li BF4 (0.14)	Lorenz 2022 ^{S8}
EMIM TFSI 1	EMIM TFSI (0.938) Li TFSI (0.062)	Gouverneur 2018 ^{S10}
EMIM TFSI 2	EMIM TFSI (0.879) Li TFSI (0.121)	Gouverneur 2018 ^{S10}
EMIM TFSI 3	EMIM TFSI (0.9) Li TFSI (0.1)	Lorenz 2022 ^{S8}
EMIM TFSI 4	EMIM TFSI (0.86) Li TFSI (0.14)	Lorenz 2022 ^{S8}
EMIM TFSI 5	EMIM TFSI (0.7) Li TFSI (0.3)	Lorenz 2022 ^{S8}
EMIM FSI 1	EMIM FSI (0.9) Li FSI (0.1)	Lorenz 2022 ^{S8}
EMIM FSI 2	EMIM FSI (0.86) Li FSI (0.14)	Lorenz 2022 ^{S8}
EMIM FSI 3	EMIM FSI (0.7) Li FSI (0.3)	Lorenz 2022 ^{S8}
Pyr12O1 TFSI	Pyr12O1 TFSI (0.6) Li TFSI (0.4)	Lorenz 2022 ^{S8}
Pyr12O1 FTFSI 1	Pyr12O1 FTFSI (0.9) Li FTFSI (0.1)	Brinkkötter 2021 ^{S11}
Pyr12O1 FTFSI 2	Pyr12O1 FTFSI (0.8) Li FTFSI (0.2)	Brinkkötter 2021 ^{S11}
Pyr12O1 FTFSI 3	Pyr12O1 FTFSI (0.7) Li FTFSI (0.3)	Brinkkötter 2021 ^{S11}
Pyr12O1 FTFSI 4	Pyr12O1 FTFSI (0.6) Li FTFSI (0.4)	Brinkkötter 2021 ^{S11}
Pyr14 TFSI 1	Pyr14 TFSI (0.9) Li TFSI (0.1)	Lorenz 2022 ^{S8}
Pyr14 TFSI 2	Pyr14 TFSI (0.86) Li TFSI (0.14)	Lorenz 2022 ^{S8}
Pyr14 FSI 1	Pyr14 FSI (0.9) Li FSI (0.1)	Lorenz 2022 ^{S8}
Pyr14 FSI 2	Pyr14 FSI (0.86) Li FSI (0.14)	Lorenz 2022 ^{S8}

The partial molar volumes of the ions are the same as in table S2 since they are assumed to be concentration-independent. For Li^+ the ionic radius of lithium (76 pm)^{S12} was taken to calculate the volume in spherical approximation as $v_{\text{Li}} = 1.11 \cdot 10^{-6} \text{ m}^3/\text{mol}$. Table S4 lists the conductivities measured by impedance spectroscopy as well as the transference numbers calculated from eq. (44).

The data shown in fig. 5 is listed here in table S5. The volume-based Li transference numbers t_{Li}^v are calculated from eq. (41) and the mass-based transference numbers t_{Li}^m from eq. (42). The species-based transference numbers t_{Li}^s are in the common anion frame of reference and calculated via the corresponding transformation rule, eq. (43).

Table S4: List of conductivities and eNMR-based transference numbers for the systems with three constituents calculated from eq. (44).

System	Conductivity κ in S/m	Transference numbers		
		lithium $t_{\text{Li}}^{\text{eNMR}}$	cation t_{+}^{eNMR}	anion t_{-}^{eNMR}
EMIM BF4 1	1.230 ± 0.123	-0.019 ± 0.004	0.526 ± 0.115	0.486 ± 0.101
EMIM BF4 2	1.080 ± 0.108	-0.039 ± 0.007	0.538 ± 0.127	0.459 ± 0.091
EMIM BF4 3	0.756 ± 0.038	-0.09 ± 0.02	0.438 ± 0.218	0.614 ± 0.188
EMIM TFSI 1	0.653 ± 0.065	-0.025 ± 0.007	0.485 ± 0.119	0.462 ± 0.108
EMIM TFSI 2	0.542 ± 0.054	-0.035 ± 0.005	0.592 ± 0.097	0.321 ± 0.107
EMIM TFSI 3	0.550 ± 0.028	-0.035 ± 0.015	0.790 ± 0.140	0.342 ± 0.078
EMIM TFSI 4	0.450 ± 0.023	-0.073 ± 0.014	0.576 ± 0.107	0.398 ± 0.160
EMIM TFSI 5	0.171 ± 0.005	-0.13 ± 0.03	0.732 ± 0.108	0.527 ± 0.080
EMIM FSI 1	1.189 ± 0.060	-0.022 ± 0.007	0.653 ± 0.074	0.496 ± 0.096
EMIM FSI 2	1.061 ± 0.053	-0.024 ± 0.010	0.548 ± 0.039	0.606 ± 0.175
EMIM FSI 3	0.715 ± 0.022	-0.08 ± 0.05	0.386 ± 0.140	0.670 ± 0.221
Pyr12O1 TFSI	0.024 ± 0.001	-0.14 ± 0.03	0.544 ± 0.108	0.563 ± 0.139
Pyr12O1 FTFSI 1	0.450 ± 0.009	-0.025 ± 0.004	0.343 ± 0.041	0.478 ± 0.057
Pyr12O1 FTFSI 2	0.251 ± 0.005	-0.063 ± 0.011	0.361 ± 0.043	0.539 ± 0.065
Pyr12O1 FTFSI 3	0.128 ± 0.003	-0.091 ± 0.015	0.494 ± 0.059	0.618 ± 0.074
Pyr12O1 FTFSI 4	0.068 ± 0.001	-0.098 ± 0.017	0.462 ± 0.055	0.604 ± 0.072
Pyr14 TFSI 1	0.146 ± 0.007	-0.040 ± 0.008	0.538 ± 0.041	0.615 ± 0.137
Pyr14 TFSI 2	0.114 ± 0.006	-0.053 ± 0.012	0.520 ± 0.042	0.608 ± 0.082
Pyr14 FSI 1	0.343 ± 0.031	-0.047 ± 0.010	0.506 ± 0.144	0.800 ± 0.277
Pyr14 FSI 2	0.337 ± 0.038	-0.05 ± 0.02	0.471 ± 0.121	0.909 ± 0.246

Table S5: List of Li transference numbers in the volume-, mass- and species-based reference frames calculated from eqs. (41) to (43).

System	Transference numbers		
	t_{Li}^v	t_{Li}^m	t_{Li}^s
EMIM BF4 1	-0.029 ± 0.006	-0.022 ± 0.003	-0.001 ± 0.008
EMIM BF4 2	-0.059 ± 0.011	-0.047 ± 0.007	-0.005 ± 0.014
EMIM BF4 3	-0.11 ± 0.03	-0.09 ± 0.03	-0.003 ± 0.05
EMIM TFSI 1	-0.021 ± 0.005	-0.013 ± 0.005	0.003 ± 0.013
EMIM TFSI 2	-0.042 ± 0.006	-0.027 ± 0.008	0.004 ± 0.018
EMIM TFSI 3	-0.049 ± 0.021	-0.033 ± 0.015	-0.001 ± 0.023
EMIM TFSI 4	-0.074 ± 0.014	-0.054 ± 0.019	-0.016 ± 0.037
EMIM TFSI 5	-0.13 ± 0.03	-0.07 ± 0.03	0.03 ± 0.05
EMIM FSI 1	-0.033 ± 0.011	-0.016 ± 0.008	0.028 ± 0.017
EMIM FSI 2	-0.024 ± 0.010	0.001 ± 0.016	0.063 ± 0.035
EMIM FSI 3	-0.04 ± 0.02	0.01 ± 0.06	0.12 ± 0.11
Pyr12O1 TFSI	-0.14 ± 0.03	-0.06 ± 0.05	0.08 ± 0.09
Pyr12O1 FTFSI 1	-0.023 ± 0.004	-0.008 ± 0.005	0.023 ± 0.010
Pyr12O1 FTFSI 2	-0.055 ± 0.009	-0.021 ± 0.012	0.045 ± 0.024
Pyr12O1 FTFSI 3	-0.091 ± 0.016	-0.027 ± 0.020	0.094 ± 0.038
Pyr12O1 FTFSI 4	-0.093 ± 0.016	-0.007 ± 0.024	0.143 ± 0.046
Pyr14 TFSI 1	-0.038 ± 0.008	-0.016 ± 0.010	0.022 ± 0.022
Pyr14 TFSI 2	-0.050 ± 0.012	-0.019 ± 0.011	0.034 ± 0.024
Pyr14 FSI 1	-0.046 ± 0.010	-0.023 ± 0.014	0.033 ± 0.038
Pyr14 FSI 2	-0.04 ± 0.02	-0.01 ± 0.02	0.08 ± 0.06

References

- (S1) Schammer, M.; Horstmann, B.; Latz, A. Theory of Transport in Highly Concentrated Electrolytes. *Journal of the Electrochemical Society* **2021**, *168*, 026511.
- (S2) Goyal, P.; Monroe, C. W. New Foundations of Newman's Theory for Solid Electrolytes: Thermodynamics and Transient Balances. *Journal of The Electrochemical Society* **2017**, *164*, E3647–E3660.
- (S3) Newman, J.; Tiedemann, W. Porous-electrode theory with battery applications. *AIChE Journal* **1975**, *21*, 25–41.
- (S4) Horstmann, B.; Danner, T.; Bessler, W. G. Precipitation in aqueous lithium–oxygen batteries: a model-based analysis. *Energy Environ. Sci.* **2013**, *6*, 1299–1314.
- (S5) Stamm, J.; Varzi, A.; Latz, A.; Horstmann, B. Modeling nucleation and growth of zinc oxide during discharge of primary zinc-air batteries. *Journal of Power Sources* **2017**, *360*, 136–149.
- (S6) Schmitt, T.; Arlt, T.; Manke, I.; Latz, A.; Horstmann, B. Zinc electrode shape-change in secondary air batteries: A 2D modeling approach. *Journal of Power Sources* **2019**, *432*, 119–132.
- (S7) Schmitt, T.; Latz, A.; Horstmann, B. Derivation of a local volume-averaged model and a stable numerical algorithm for multi-dimensional simulations of conversion batteries. *Electrochimica Acta* **2020**, *333*, 135491.
- (S8) Lorenz, M.; Kilchert, F.; Nürnberg, P.; Schammer, M.; Latz, A.; Horstmann, B.; Schönhoff, M. Local Volume Conservation in Concentrated Electrolytes Is Governing Charge Transport in Electric Fields. *The Journal of Physical Chemistry Letters* **2022**, *13*, 8761–8767.

- (S9) Gouverneur, M.; Kopp, J.; Van Wüllen, L.; Schönhoff, M. Direct determination of ionic transference numbers in ionic liquids by electrophoretic NMR. *Physical Chemistry Chemical Physics* **2015**, *17*, 30680–30686.
- (S10) Gouverneur, M.; Schmidt, F.; Schönhoff, M. Negative effective Li transference numbers in Li salt/ionic liquid mixtures: Does Li drift in the "wrong" direction? *Physical Chemistry Chemical Physics* **2018**, *20*, 7470–7478.
- (S11) Brinkkötter, M.; Mariani, A.; Jeong, S.; Passerini, S.; Schönhoff, M. Ionic Liquid in Li Salt Electrolyte: Modifying the Li⁺ Transport Mechanism by Coordination to an Asymmetric Anion. *Advanced Energy and Sustainability Research* **2021**, *2*, 2000078.
- (S12) Shannon, R. D. Revised effective ionic radii and systematic studies of interatomic distances in halides and chalcogenides. *Acta Crystallographica Section A* **1976**, *32*, 751–767.